

Laboratory Research

Use of an Artificial Lymphatic System During Carboplatin Infusion to Improve Canine Osteosarcoma Blood Flow and Clinical Response

Gene R. DiResta, PhD,¹ Sean W. Aiken, DVM,² Holly K. Brown, MD,¹
Philip J. Bergman, DVM, PhD,² Ann Hohenhaus, DVM,² E. J. Ehrhart, DVM, PhD,³
Keith Baer, DVM,² and John H. Healey, MD¹

¹Orthopaedic Surgical Service, Memorial Sloan Kettering Cancer Center, 1275 York Avenue, New York, New York 10021-6007

²The Animal Medical Center, 510 E 62nd Street, New York, New York 10021

³College of Veterinary Medicine and Biomedical Science, Colorado State University, Ft. Collins, Colorado 80523

Background: The artificial lymphatic system (ALS), a mechanical system designed to reduce increased interstitial fluid pressure in solid tumors and enhance the delivery of chemotherapy, was evaluated within a randomized clinical trial treating spontaneously occurring canine appendicular osteosarcoma (OS), a tumor similar to its human OS counterpart.

Methods: An ALS was investigated for its ability to increase OS blood flow and increase uptake of intravenously administered carboplatin.

Results: Blood flow increased by 314% in tumors with active ALS drains versus 126% in control tumors ($P < .03$). Tumor carboplatin uptake increased by 51% after drain activation ($P = .07$). Microvascular density (MVD) was measured in tumors after surgical amputation and in corresponding bone regions in a cohort of normal dogs. The OS tumors had equivalent MVD as normal bone, and MVD was higher in the humerus than the femur ($P < .03$) in both tumor and normal bone. Median survival between the ALS-treated and control cohorts was not different despite increased drug uptake or ALS manipulation. Compared with historic controls, ALS drain insertion into tumors to reduce interstitial fluid pressure did not worsen the prognosis.

Conclusions: The findings in canine spontaneously occurring OS indicate that an ALS may be of value as a chemotherapy adjunct for enhancing the delivery of chemotherapy to tumor interstitium.

Key Words: Osteosarcoma—Carboplatin—Blood flow—Interstitial fluid pressure—Microvessel density—Canine—Artificial lymphatic system.

Increased interstitial fluid pressure (IFP) is assumed to impede chemotherapy transport into tumor interstitium¹ and contributes to the interstitial hypoxic and acidotic conditions² that reduce the efficacy of chemotherapy and radiotherapy.³ We have observed

increased IFP and reduced tracheal blood flow (TBF) in rat,⁴ human brain,⁵ human bone tumors,⁶ and most recently in spontaneously occurring dog tumors.⁷ In fact, every solid tumor studied by our group^{4–6} displayed increased IFP. Therefore, strategies that lower IFP and increase TBF should increase the interstitial delivery of chemotherapy and its local effectiveness.

Pharmacologic⁸ and mechanical² approaches to reduce tumor IFP have enhanced chemotherapy uptake and resulted in tumor shrinkage. However, the pharmacologic approach⁸ identified the following: (1) IFP-reducing drugs result in a wide variability of response,

Received November 10, 2006; accepted January 26, 2007;
published online: May 15, 2007.

Address correspondence and reprint requests to: Gene R. DiResta, PhD; E-mail: direstag@mskcc.org

Published by Springer Science+Business Media, LLC © 2007 The Society of Surgical Oncology, Inc.

(2) it is hard to determine how soon after IFP reduces one should administer chemotherapy, and (3) local delivery of IFP-reducing drugs is associated with increased local edema. The artificial lymphatic system (ALS) is a mechanical approach that lowers local IFP by aspirating small amounts of fluid within the tumor interstitium associated with the increased IFP.^{2,9} The technique can be controlled, it has a reproducible effect, and its influence is limited to tumor regions surrounding the ALS drains. Introductory studies were performed by using ALS with a rat xenograft dual-tumor model. A drain was applied to one tumor, and the second served as drain-free control. After systemic delivery of chemotherapy, ALS-drained tumors had decreased IFP, increased TBF, and greater drug uptake that shrank the tumor faster than control tumor.⁹ On the basis of those findings, the ALS system was redesigned for use in human tumors¹⁰ and evaluated in a veterinary clinical trial performed at The Animal Medical Center (AMC) to investigate the efficacy of an ALS to enhance carboplatin delivery into spontaneously occurring appendicular osteosarcoma (OS) in large-breed dogs.

Canine appendicular OS was selected because its natural histology and response to neoadjuvant chemotherapy are similar to human OS.¹¹ Further, the appendicular location allowed safe access and monitoring capability. Clinical methodology developed from the veterinary trial could be applied to a human solid tumor clinical trial. Pretrial measurements of canine OS IFP determined that IFP, although higher than in soft tissue tumors, was similar to values reported for human OS.⁷

The quantity and distribution of systemically delivered molecules into tissue interstitium are directly related to the tissue's microvascular density (MVD) because molecular transport occurs across a capillary's luminal surface as well as via blood flow. Therefore, MVD measurements were performed on tumor and normal tissue regions that were removed from amputated limbs to characterize and compare the regions' capillary distribution.

Two hypotheses were tested: first, ALS drainage of canine appendicular OS will increase its blood flow, tissue Po₂, and uptake of intravenously administered carboplatin; and second, canine OS MVD is less than the MVD of normal bone from equivalent sites.

MATERIALS AND METHODS

The Memorial Sloan Kettering Cancer Center (MSKCC) and the AMC Institutional Animal Care

and Use Committees approved all procedures in this study. Dog owners gave written informed consent for all procedures performed on their pets.

The study had two stages: first, two characterization components were performed with normal (MSKCC) and tumor-bearing dogs (AMC); and second, the clinical trial was performed (AMC). The normal component measured reference values for IFP, capillary blood flow, Po₂, and pH of bone and muscle in four dogs scheduled for euthanasia from studies that did not influence their front legs. The tumor-bearing component, performed in two dogs with appendicular OS, evaluated the ALS drain design, its effect on tumor IFP, and its blood flow dynamics.

Stage 2 was performed as a randomized clinical trial. The ALS effect's primary outcome measures, TBF and Po₂, were continuously recorded in tumor regions before and after ALS drain insertion during the tumor decompression, vacuum application, and chemotherapy administration periods. Tumor drug levels were measured from tissue sampled in regions adjacent to the ALS drain. IFP and pH were not measured to reduce probing the tumor and weakening the host bone.

Clinical outcome was assessed by comparing serum alkaline phosphatase levels (ALP), measured before and 1 month after surgery¹² by measuring the percentage of tumor necrosis¹³ in specimens amputated 2 weeks after receiving ALS-chemotherapy treatment, and by performing Kaplan-Meier survival analysis to compare overall survival of dogs treated with the ALS-adjunct versus AMC-historic treatments.¹⁴

MVD measurements were performed by Colorado State University on tumor resection specimens. Tumor MVD was compared with MVD in equivalent sites from normal femur and humeri collected from five normal Colorado State University dogs, similar in size to the AMC dogs, euthanized after accidental injury.

Artificial Lymphatic System

The ALS^{2,10} fabricated in MSKCC's Instrument Shop, included a multiport manifold that distributed vacuum via 1/16-inch inner-diameter Tygon S-50-HL tubing (Saint-Gobain Plastics, Akron, OH) to a network of drains inserted into the tumors' central region. Drain length reflected the tumors' thickness at insertion locations. A vacuum of -80 to -100 mm Hg, sufficient to aspirate fluid without damaging tumor, was applied to the manifold.

Common Procedures

Before surgery, dogs underwent a physical examination, complete blood count and biochemical profile, and three thoracic-view radiographs that included dorsoventral, right lateral, and left lateral views to look for lung metastases. Anterior-posterior and lateral radiographs of the tumor were used to identify locations for probes and drain, and tumor volume was estimated throughout treatment. Dogs were preanesthetized with hydromorphone (.1 mg/kg), induced with Valium (.3 mg/kg)-propofol (4 mg/kg), intubated, and anesthetized with 1% to 2% isoflurane in 100% O₂. Two venous catheters were placed into superficial limb veins for delivery of maintenance fluids and chemotherapy. Cardiac function and hemoglobin O₂ saturation were continuously monitored by electrocardiogram and lingual pulse oximetry, respectively, with a Vet/Ox Plus 4800 (Heska Corp., Ft. Collins, CO). A rectal probe monitored core temperature. By use of aseptic surgical techniques, the tumor's pseudocapsule was exposed and the ALS drain, laser Doppler blood flow (LDF) probe, and Po₂ electrode were inserted in its midsection. Drain placement was facilitated by a 9-gauge bone biopsy instrument. We observed that 3-cm-long drains traversed the entire width of the tumors' central region. An 18-gauge needle was used to introduce the smaller diameter measurement probes through the rigid tumor matrix to minimize probe damage. Measurement probes were positioned opposite the drain, 1 cm away and approximately 180° opposite each other.

Instrumental Measurement Techniques

Real-time capillary blood flow was measured by a Trimflo (1.0 mm outer diameter) parenchymal LDF probe connected to the Laserflo BPM2 Blood Perfusion Monitor (Vasamedics, St. Paul, MN).²

Tissue Po₂ was measured with a model 768-22 polarographic (.7 mm outer diameter) oxygen electrodes (Diamond General, Ann Arbor, Mich.). This electrode is a 25-μm gold-plated platinum cathode covered with an O₂-permeable membrane. A sintered Ag/AgCl electrode, used as the reference anode (In Vivo Metric, Healdsburg, CA), was wrapped in saline-soaked gauze and placed in the dogs' mouths. The oxygen and reference electrodes were connected to the SG-2 Polarograph (MicroFlow Associates, Pleasantville, NY). A polarization voltage of -.7 V (direct current) was applied across the electrodes. Before insertion and after use, the oxygen electrode underwent a two-point calibration by using 100% N₂ and 10% O₂-90% N₂ saturated, pH 7.4,

phosphate-buffered saline solutions at 37°C. A linear correction model corrected drift; data were considered unusable when calibration values differed by > 20%.

IFP was measured with a Wick-in-Needle probe² and a Camino 420 Pressure monitor. Electrocardiogram was acquired with the Vet/Ox Plus monitor. pH was measured with a 20-gauge combination pH electrode (Diamond General) connected to a Denver Instruments pH meter (Denver, CO) calibrated with pH 4 and 7.0 buffers at 37°C.

The perfusion, polarograph, pressure, and electrocardiogram monitor analog outputs were continuously acquired by a PC analog input/output data acquisition system (Dataq Instruments, Akron, OH). The pH meter's serial output was acquired into an Excel spreadsheet using Winwedge Pro software (TAL Technology, Philadelphia, PA).

Tumor Volume Estimation

Tumors were assumed to be solid ellipsoids whose volume was estimated by the following formula:

$$\text{volume} = [4/3 \cdot \pi \cdot A \cdot B \cdot C \cdot (1 + f_a)^{-3}]$$

where A = [(AP length + L length)/2]; B = (AP width/2), C = (L width/2); and f_a = film amplification factor (.12 in this study). AP and L refer to the anterior-posterior and lateral plane film views of the tumor leg; and length and width refer to digital caliper measurements (cm) of the tumors' maximum length and width within the film views.

Microvessel Density Analysis

Immunohistochemical staining of tumor and normal bone specimens was performed with an automated stainer (Discovery System, Ventana Medical Systems; Tucson, AZ). All reagents (Ventana Medical Systems, Tucson, AZ) were incubated at 37°C. Briefly, 4-μm sections were cut and mounted on positively charged slides, the paraffin removed, and the sections rehydrated with descending alcohol concentrations to buffer. Antigen retrieval was with protease 1 incubation for 16 minutes. The sections were incubated for 12 hours with a monoclonal anti-CD31 antibody at a dilution of 1:100 (Dako, Carpinteria, CA, clone JC70A). A prediluted, universal biotinylated secondary antibody and a diaminobenzidine (DAB) MAP detection kit (Ventana Medical Systems, Tucson, AZ) were used to detect the immunoreactive complexes. The slides were then counterstained with Mayer hematoxylin.

Image analysis was performed by KS-400 system software (Carl Zeiss, Thornwood, NY). Five semi-random hot zone images were taken for each specimen with a Carl Zeiss Axioplan 2 imaging scope coupled with an AxioCam HRc Carl Zeiss camera. By using a threshold feature, DAB-stained pixels were converted to white and unstained pixels to black. MVD was determined as the number of white pixels over total pixels. The camera exposure and threshold levels were constant for the acquisition and analysis of all images.¹⁵

Stage 1: Characterization

Normal Dogs

IFP, blood flow, pH, and Po₂ were measured in the left proximal humeri and adjacent triceps muscles of four normal dogs scheduled for euthanasia. While the dog was under the anesthesia described above, the humerus was exposed by blunt dissection. Entry holes were made into the bone cortex by using a 1.22-mm-diameter Kirshner wire to accommodate the probes. After signals stabilized, the probes were removed and placed into adjacent triceps muscle. Dogs were euthanized by intravenous sodium pentothal.

Tumor-Bearing Dogs

Two dogs with proximal humeral OS and scheduled for amputation were used in this component. The LDF and Wick-in-Needle probe probes were positioned near the tumor center 1 cm from each other. Figure 1 is a photomontage from the dog B study showing the ALS equipment and its implementation. Figures 2a and b show the drain, IFP, and LDF locations in the two dog tumors. IFP, TBF, and electrocardiogram signals were recorded as vacuum was applied. After the signals stabilized, the vacuum was turned off. This sequence was repeated several times over a 30-minute period. Amputation was performed when data acquisition ended. From January 2000 to April 2003, dogs with histologically confirmed appendicular OS were recruited into the clinical trial. Dogs were excluded if they had previously received chemotherapy or radiotherapy, or if metastasis was detected on their chest radiographs. Two therapeutic protocols were used during this period. The original included a 2-week observation period after measurements and drug administration before amputation. The final protocol eliminated the observation period matching the typical treatment for dog OS.¹⁶ All dogs received one LDF probe, one Po₂ electrode, and one drain positioned in the tumors' central region. To facilitate monitoring

TBF and Po₂ before tumor decompression, the LDF probe was positioned first, followed by the Po₂ electrode and finally the ALS drain.

Procedures

After the intratumoral LDF and Po₂ signals stabilized and the dog was hemodynamically stable, it was randomly assigned to receive -80 mm Hg vacuum or 0 mm Hg (control). Carboplatin (300 mg/m²) (Bristol-Meyers-Squibb, Princeton, NJ) infusion started 10 minutes after the LDF signal stabilized after vacuum application, or 20 minutes after drain insertion in control dogs. Administration was via infusion pump over 10 minutes. Data acquisition was stopped 10 minutes after infusion ended. Tumor, taken from regions adjacent to the drain, and arterial blood plasma were flash frozen in liquid N₂ and stored at -26°C. The specimens' platinum content was analyzed by atomic absorption spectroscopy by the MSKCC Clinical Chemistry Laboratory. Carboplatin levels were computed by multiplying the measured platinum levels with the stoichiometric ratio of carboplatin to platinum (i.e., 371.25/195.08).

Statistical Analysis

Statistical analysis was performed by SPSS software, version 12 (SPSS, Chicago, IL). The Student t-test was used with the carboplatin, blood flow, and Po₂ data; the Mann-Whitney U-test was used with the ALP and percentage of necrosis data. Kaplan-Meier analysis was used with the survival data. Log rank, Breslow, and Tarone-Ware statistics and significance tests were performed on the following four data sets: ALS with vacuum on; ALS with no vacuum; no ALS; and no treatment.

RESULTS

Stage 1: Characterization Study

Normal Dogs

Table 1 summarizes IFP, local blood flow, Po₂, and pH from the normal humeri and adjacent triceps. No statistically significant difference was observed for any parameter between bone and muscle.

Tumor-Bearing Dogs

Figures 2a and b are data recording segments from the two characterization studies. Figure 2a is from

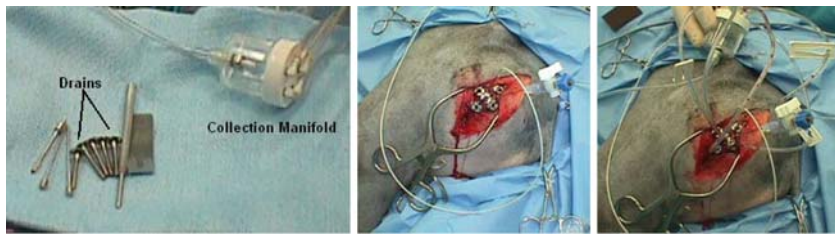


FIG. 1. Image montage of artificial lymphatic system (ALS) equipment; when inserted into tumor and when connected to house vacuum. The image set is that of dog B.

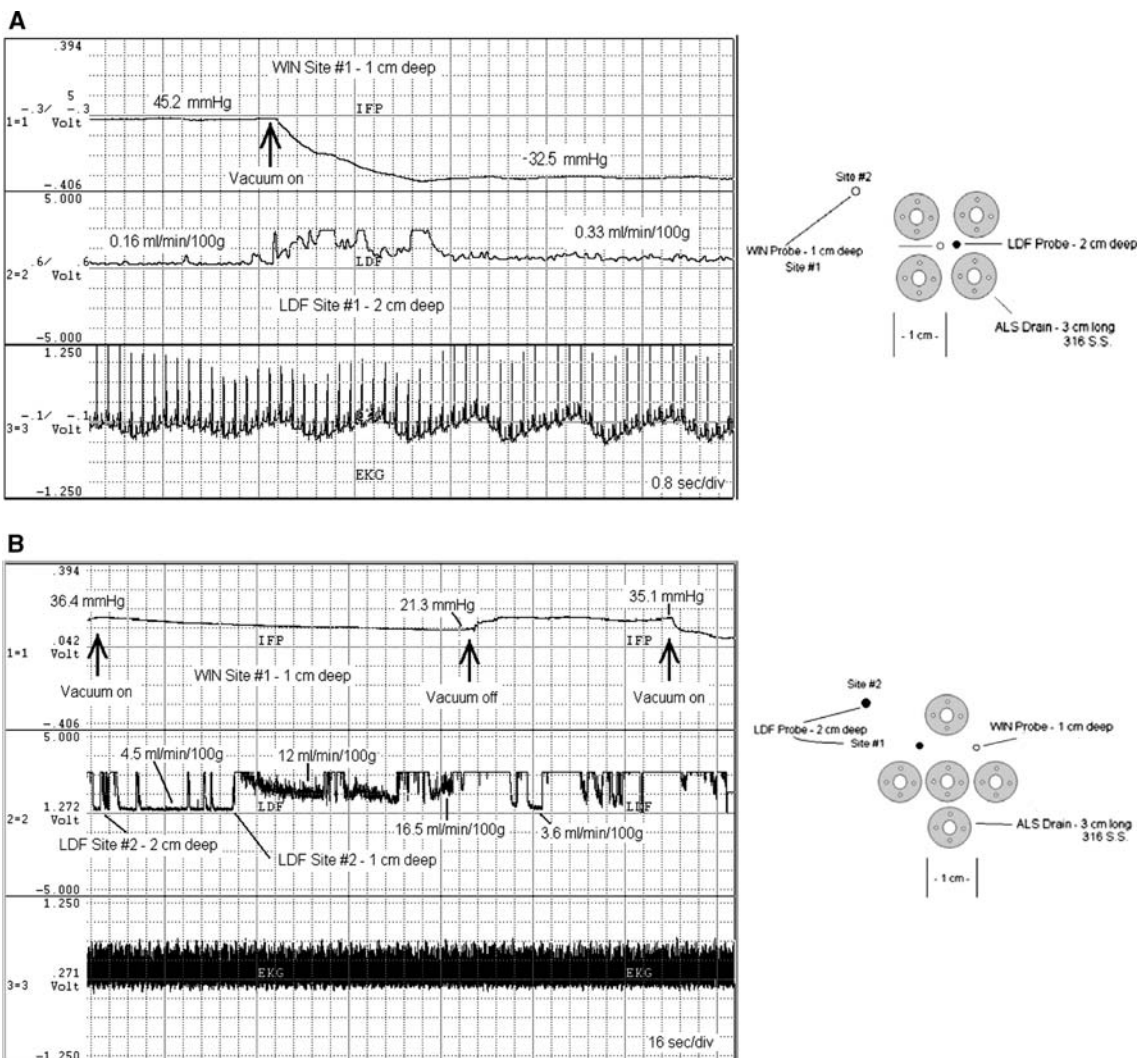


FIG. 2. Annotated data recording of interstitial fluid pressure (IFP), laser Doppler blood flow (LDF) blood flow signal, and electrocardiogram from dogs A and B. The time base for dog A is shown 20 \times faster than for dog B to visualize the faster response of LDF and IFP after vacuum application to drain. Dog A had rigid tumor matrix; dog B had compressible tumor matrix. The artificial lymphatic system (ALS) drain, LDF (solid circles), and Wick-in-Needle (WIN) (open circles) probe locations associated with the data tracings are shown to the right of the tracings. The larger circles are the suture rings surrounding the drain opening. Site numbers refer to chronological measurement locations.

the first study, an OS tumor that was rigid on palpation; Fig. 2b is from the second study, an OS tumor that was compressible on palpation. In both

figures, IFP lowered when vacuum was applied and increased when vacuum was removed. The time constant to reduce IFP from the rigid tumor was 1.5

TABLE 1. Normal dog values of Po_2 , blood flow, pH, and IFP ($n = 4$; mean \pm SEM)

Location	Po_2	Flow (mm Hg)	pH (mL/min/100 g)	IFP (mm Hg)
Left proximal humerus	166.6 \pm 39.6	3.0 \pm 2.2	7.3 \pm .1	17.2 \pm 10.0
Left triceps	161.2 \pm 29.7	6.1 \pm 1.7	7.0 \pm .2	5.8 \pm 6.3

IFP, interstitial fluid pressure.

TABLE 2. Demographics of dogs recruited into clinical trial (mean \pm SEM)

Group	Age (y)	Sex/status	Weight (kg)	Tumor location	Tumor volume (cm^3)
Vacuum treated (n = 7)	9.2 \pm .7	5 male/castrate; 2 female/spay	40 \pm 5.4	2 proximal humerus, 2 distal femur, 2 distal radius, 1 distal tibia	137.8 \pm 108.3
Non-vacuum treated (n = 7)	7.6 \pm .8	4 male/castrate; 3 female/spay	42.4 \pm 4.9	2 proximal humerus, 1 tarsus, 3 distal radius, 1 distal tibia	73.0 \pm 43.4

to 2 seconds, whereas it was 1.5 to 2 minutes for the compressible tumor. Subsequent pressure reductions were slower than the first. The LDF signal increased sharply when vacuum was first applied. This initial response reflects the movement of fluid within the matrix into the drain. The time constants associated with flow changes were 2.5 to 3.5 seconds for the rigid tumor and 2.4 to 3 minutes for the compressible tumor.

Stage 2: Clinical Trial

Fourteen dogs entered the trial (Table 2). Diagnoses of OS were confirmed by biopsy; disease of 13 dogs were osteoblastic and was fibroblastic in 1.

Tumor Blood Flow

Figure 3 summarizes the ALS influence on TBF. One vacuum-treated dog and two control dogs were excluded as a result of instrumentation malfunction. The figure presents TBF immediately before drain insertion and carboplatin infusion.

Flow significantly increased, on average, by 314% in the vacuum-treated dogs ($P < .03$). As a result of simply inserting the drain into the tumors, the average flow increased by 126% ($P < .15$). The vacuum precarboplatin group had a 48% higher mean flow than the control precarboplatin group, which was not significant ($P < .19$).

Carboplatin Uptake

Carboplatin concentration (ng carboplatin/g tissue) (mean \pm SEM) in tumor specimens was 16.6 ± 5 (vacuum treated) and 8.1 ± 2.3 (control).

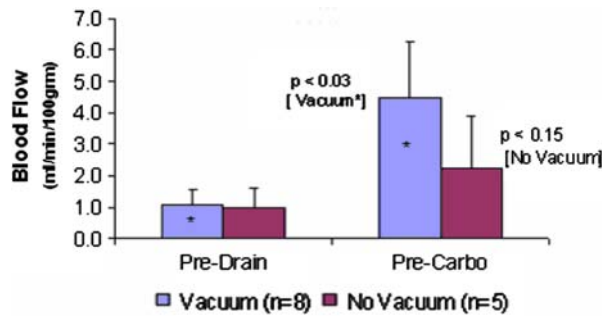


FIG. 3. Influence of artificial lymphatic system (ALS) decompression on tracheal blood flow (TBF) before drain insertion (Pre-Drain) and after a 10-minute application of vacuum to drain immediately before infusion of carboplatin (Pre-Carbo) (mean \pm SEM).

The value from one control dog was excluded because of blood contamination; data from this dog were also excluded from the blood flow analysis. The vacuum-treated group had a 51% higher concentration than the control group ($P = .07$). Plasma levels were lower in the vacuum group, 43.3 ± 7.5 mg/L, versus the control group, 50.7 ± 5.8 mg/L, but this was not statistically significant.

ALP Change and Percentage of Tumor Necrosis

Percentage changes (mean \pm SD) in serum ALP were measured in 4 vacuum-treated dogs (-20.7% \pm 46.1%) and 4 control dogs (10.2% \pm 59.7%). ALP decreased in three of the four vacuum-treated dogs and in one of the four control dogs; however, the means were not statistically different ($P = .6$). Percentage of necrosis (mean \pm SEM) was measured 2 weeks after treatment in 7 of the 10 dogs studied under the original

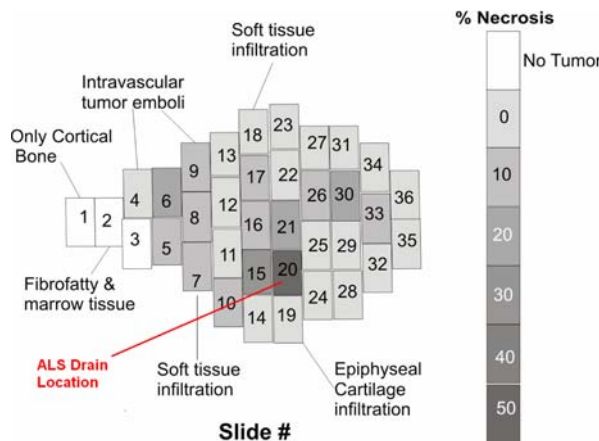


FIG. 4. Percentage of tumor necrosis map illustrating carboplatin's heterogeneous tumor response and the enhanced therapeutic effect of the region influenced by artificial lymphatic system (ALS) drainage.

protocol, 4 from the vacuum-treated group ($18\% \pm 14\%$) and 3 from the control group ($67\% \pm 29\%$); however, the means were not statistically different ($P = .21$). A percentage necrosis map from one vacuum-treated dog illustrates the heterogeneity of tumor response observed and the vacuum influence on percentage of necrosis surrounding the drain (Fig. 4).

Oxygen Tension

Po_2 (mean \pm SEM) was successfully measured in five vacuum-treated and four control dogs. Probe breakage and excessive drift of pre- and poststudy calibration values precluded data acceptance from the other dogs. Po_2 in the vacuum-treated group ($n = 5$) before drainage and before carboplatin infusion were 30.2 ± 14.9 mm Hg and 38.2 ± 19.3 mm Hg, respectively. The mean Po_2 increase, 27%, was not significant ($P = .3$). Po_2 in the control group ($n = 4$) after probe insertion and before carboplatin infusion were 46.9 ± 27.0 mm Hg and 47.0 ± 44.2 mm Hg, respectively; no Po_2 increase occurred ($P = .3$).

The average tumor Po_2 ($n = 9$) measured after drain placement was 42.1 ± 13.7 mm Hg, which was significantly lower than the average value measured in the humerus of the normal dogs, 166.6 ± 39.6 mm Hg ($P < .003$).

Microvascular Density

Mean MVDs in comparable regions of tumor and normal bone were not significantly different ($P > .16$); however, tumor and normal bone mean MVD was greater in front limb than hind limb locations

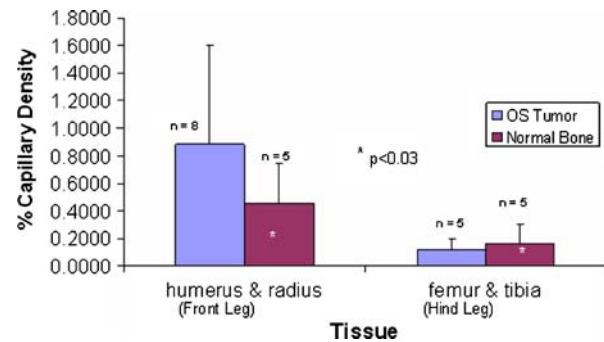


FIG. 5. Microvascular density (MVD) (mean \pm SD) in osteosarcoma and normal bone, front leg versus hind leg. The relationship for tumor and normal bone is equivalent, i.e., MVD is greater in front leg than hind leg, reflecting weight bearing of bone.

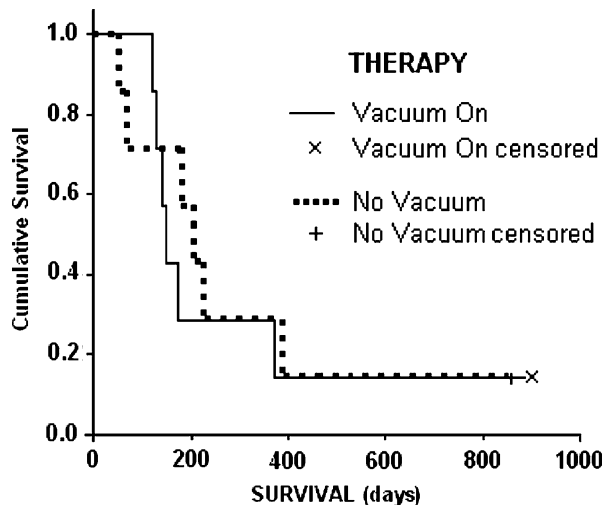


FIG. 6. Kaplan-Meier survival curves comparing both artificial lymphatic system (ALS) treatment cohorts.

(Fig. 5). A significant difference ($P < .03$) was observed between the normal femur and radius MVD.

Long-Term Survival

Survival of animals in the two ALS groups (Fig. 6) was compared with AMC historical controls.¹⁴ From 1993 to 1998, a total of 29 dogs with OS received no treatment, and 35 dogs were treated with amputation and chemotherapy. The median survival for the control (no treatment) and amputation and chemotherapy cohorts was 48 days and 380 days, respectively, whereas the median survival for the ALS vacuum-treated and ALS non-vacuum-treated groups was 148 days and 209 days, respectively.

By intent-to-treat analysis, there was no survival difference between the two ALS groups ($P > .1$).

However, a significant improvement ($P < .03$) was observed between both ALS groups and the control group (no AMC treatment). Further, there was no difference between both ALS groups and the historic AMC amputation and chemotherapy group ($P > .1$).

DISCUSSION

The central tumor regions were implanted with ALS drains because they typically have the highest IFP and lowest blood flow, Po_2 , and pH values, and this is the region where drug delivery is most compromised. IFP, TBF, Po_2 , and pH are not homogeneous within a solid tumor; rather, IFP decreases while TBF, Po_2 , and pH increase from the tumor center to its interface with normal tissue. These parametric relationships are theoretically anticipated^{1,2} and have been experimentally confirmed in rat tumors.^{2,4} We assumed that aspirating OS from its central region would influence its entire volume. However, the percentage of necrosis variability (Fig. 4) implies that ALS decompression primarily influences regions surrounding the drain, suggesting that these tumors' physical properties may be compartmentalized.

The clinical findings indicate that in OS a vacuum-activated ALS was capable of increasing regional TBF to levels that approach those measured in the proximal humeri of our normal dogs and that uptake of systemically administered carboplatin was greater than levels measured in control tumors. Although no published reports of carboplatin levels in dog OS have been identified, our values are equivalent to or greater than values published in human studies that used carboplatin to treat head and neck cancer¹⁷ and uterine and cervical cancer.¹⁸ Those studies report platinum concentrations of $1.4 \pm .03$ ($n = 11$) and 6 ± 1.3 ($n = 9$) ng Pt/mg tumor, respectively, after systemic administration of carboplatin at doses of 250 to 500 mg/m². The platinum concentrations for vacuum-treated and control OS are 8.7 ± 6.6 ($n = 7$) and 4.3 ± 3.1 ($n = 6$) ng Pt/mg tumor, respectively.

As was previously demonstrated in the rat dual tumor studies,² ALS significantly increased drug uptake over control tumors ($P < .05$). However, several factors distinguish the canine OS study from the rat dual-tumor study.² This dog study reflects the clinical situation where spontaneously occurring disease within heterogeneous patient and tumor populations are used to evaluate the efficacy of a treatment. The rat studies used dual xenograft tumors of identical

size (2 cm diameter) and characteristics; each rat served as its own control. The dog OS locations, matrix characteristics, and dimensions varied between and within dogs in the two trial cohorts. These structural parameters influenced the rate and extent of the drainage effect (Fig. 2) and reduced the power of our findings. Abe et al.¹⁹ demonstrated that tumor size influences the heterogeneity of response in tumors after chemotherapy.

Blood flow and Po_2 values measured in the normal bone were higher than those measured in the OS central tumor regions. The mean value for normal dog humeral blood flow, 3.0 ± 2.2 mL/min/100 g, was obtained by LDF, a real-time local measurement technique. It is similar to values reported for normal dog humeral blood flow measured by a microsphere technique, i.e., 3.57 mL/min/100 g,²¹ which is a whole-organ averaging technique. Similarly, normal dog proximal humeral Po_2 and pH obtained with *in situ* polarographic and pH microelectrodes, i.e., 166.6 ± 39.6 mm Hg and $7.3 \pm .1$, respectively, are equivalent to values reported for normal dog humeral diaphysis, i.e., 135 mm Hg and 7.43, for comparable anesthesia mixtures²⁰ by using anaerobically drawn blood from the humerus and measured with a blood gas analyzer. The similarity of our flow, Po_2 , and pH values to published values supports the validity of our measurement technology and the regional values we report herein.

Li et al.²¹ report that mean humeral cortical flow is far higher than mean femoral cortical flow, i.e., 2.9 mL/min/100 g, reflecting increased weight bearing. In large-breed dogs, such as those we enrolled onto our clinical trial, weight distribution is 60% to 70% front limbs, 40% to 30% hind limbs.^{22,23} This relationship is consistent with our observations that humeral MVD is far greater than femoral MVD and suggests that the variation associated with the mean blood flow we report are related in part to the tumors' anatomic locations (Fig. 5).

The neoadjuvant therapeutic approach initially used in this clinical trial, although similar to human therapy,²⁴ is not always used for dog OS.¹⁶ Despite the increased carboplatin uptake, some tumors continued to grow during the interval between administration and amputation. Further, the extent of tumor necrosis findings, although from a small cohort, indicated that there was no treatment advantage in the vacuum-treated versus control dogs. The lack of tumor shrinkage forced a decision to modify the protocol to match typical treatment for dog OS.

The improved drug delivery in ALS vacuum-treated OS tumors conferred no survival advantage over

the ALS non–vacuum-treated group; both groups' survival was equivalent to a historical treatment group of amputation and chemotherapy. A recent study²⁵ that used amputation followed by carboplatin (175 mg/m² intravenously, day 1) and doxorubicin (15 mg/m² intravenously, day 2) resulted in a median survival time of 235 days (n = 24), which is equivalent to the AMC amputation and chemotherapy historic cohort, as well as our ALS groups that were treated with carboplatin. The lack of survival differences between both ALS-treated groups and the historic treatment group suggests that drain insertion into tumors did not expose the dog to additional risk from tumor cells escaping into the circulation. ALP changes support this observation because 2 to 4 weeks after amputation, ALP changes reflecting systemic disease burden¹² were lower in the vacuum-treated dogs. Because amputation was the planned local therapy, no comment can be made about how ALS may influence limb-sparing local resection surgery, an important issue in managing human OS.

The image analysis approach used for the MVD analysis has been extensively used and published in both dog^{26,27} and human tumor MVD analysis.²⁸ We adapted the method of Kent et al.,²⁷ who analyzed MVD in canine thyroid neoplasms with CD31 and factor VIII-related antigen immunohistochemistry and identified different subsets of vessels with the two markers that suggested that CD31 identified both established and new vessels; factor VIII-related antigen identified established vessels. Other studies determining tumor vascularity in hot spots by this computerized method as compared with manual counts have demonstrated that image analysis is more reliable and objective.^{15,28–30}

The tumors' continued growth after chemotherapy and their equivalent MVD with normal tissue prompted us to investigate other factors that could reduce the chemotherapy's effectiveness. A Spälteholz technique was used to investigate the microvascular distribution of dog appendicular OS.³¹ This method visualized the tumor's patent capillaries by infusing Higgins India ink into the primary artery of an amputated tumor-bearing limb. The ink's 3.8- to 5.9-μm-diameter carbon particles³² move into vessels whose luminal diameters are less than the ink particle diameter. When the tissue is sectioned and clarified, the presence of the particles indicate the tissues' capillary distribution. We observed that dog OS has a heterogeneous distribution of microvessels and seems less vascularized than normal adjacent bone. However, immunohistologic measures indicate that MVD was no different in OS and normal tissue in our study

dogs. Taken together, the Spälteholz and histologic findings suggest that canine OS displays a MVD equivalent to normal bone, but that its capillary lumen diameters preclude the entry of particles or cells whose diameter is >4 to 5 μm. The reduced internal diameter may be attributed to tumor compression of the capillary vessels.³³ This observation may explain the modest Po₂ increase after ALS drainage. We propose that although the ALS reduced IFP and increased TBF and drug uptake, the absence of an adequate capillary distribution network reduced the effectiveness of the single-drain ALS used in this study. It remains to be determined how these anatomic and physiologic changes translate into heterogeneous response to chemotherapy depicted in Fig. 3 or tumor progression.³⁴

Recent cell culture studies performed with human OS lines grown under hydrostatic pressures equivalent to dog OS IFP determined that at least some OS are more proliferative³⁵ and sensitive to chemotherapeutic agents than cells grown at atmospheric pressure.³⁶ The findings suggest that neoadjuvant chemotherapy should be more effective if OS transport barriers were reduced to enable therapeutically important levels of drug to enter the tumor interstitium.

The clinical use for this technology has theoretical benefits and risks, and the technique will need to be adapted to the local tumor situation. Increasing blood flow within the tumor's patent vessels by using an ALS may be a useful adjunct for the local treatment of solid tumors. Larger and more heterogeneous tumors cannot be adequately treated with a single drain. A multidrain ALS would be needed to enhance drug delivery and efficacy. It was not used in this dog trial because more drains would have weakened the bone further and increased the risk of fracture. Finite element mathematical modeling that considers tumor matrix characteristics and dimensions is currently being investigated to determine the number and optimal placement of drains to treat tumors. If multiple drains are used clinically, potential problems such as cancer seeding of the drain track must be prevented. Notably, such complications were not seen in this trial.

Drug levels and distribution will reflect the distribution of patent vasculature; however, the clinical success of any ALS depends on the effectiveness of the chemotherapeutic agent for killing or shrinking the tumor. Potentially, this method could permit narrower surgical margins, preserve more normal articular and muscular tissue, and improve the

functional result of limb-sparing surgery or radiation. It may also be useful in shrinking liver, head and neck, brain, and nonresectable tumors. Although better systemic therapy is needed to improve overall survival, enhanced local control is always desirable.

ALS drainage of tumors, although influenced by tumor matrix characteristics, increased TBF and carboplatin uptake, and corroborated previous rat tumor drug uptake findings. Unexpectedly, MVD was equivalent in OS and normal bone.

Increased drug concentration and TBF did not translate into a better clinical outcome in this tumor. The capillary network within canine OS causes inadequate delivery and heterogeneous distribution of drug to and throughout the tumor. For these tumors, a single drain ALS is of minimal value and will only influence regions in the vicinity of the drain. The multidrain ALS (Figs. 1 and 2), rather than the single-drain ALS, may be more efficacious in treating large tumors.

ACKNOWLEDGMENTS

Supported by National Institutes of Health grant CA7884494 and the Yurman and Perlman Limb Preservation Funds.

REFERENCES

- Baxter LT, Jain RK. Transport of fluid and macromolecules in tumors: I. Role of interstitial pressure and convection. *Microvasc Res* 1989; 37:77–104.
- DiResta GR, Lee J, Healey JH, et al. The artificial lymphatic system: a new approach to reduce interstitial hypertension and increase blood flow, pH and Po_2 in solid tumors. *Ann Biomed Eng* 2000; 28:543–55.
- Weinmann M, Belka C, Plasswilm L. Tumour hypoxia: impact on biology, prognosis and treatment of solid malignant tumors. *Oncologie* 2004; 27:83–90.
- DiResta GR, Lee J, Larson SM, et al. Characterization of neuroblastoma xenograft in rat flank: I. Growth, interstitial fluid pressure and interstitial fluid velocity distribution profiles. *Microvasc Res* 1993; 46:158–77.
- Arbit E, Lee J, DiResta GR. (1994) Interstitial hypertension in human brain tumors: possible role in peritumoral edema formation. In: Nagai H, Kamiya K, Ishii S (eds) *Intracranial Pressure*. Springer-Verlag, Nagoya, Japan, pp 610–4.
- Healey JH and DiResta GR. Measurement of interstitial fluid pressure and blood flow in human bone tumors and adjacent normal tissue. Paper presented at: Orthopedic Research Society, 44th Annual Meeting; March 16–19, 1998; New Orleans, LA.
- Zachos TA, Aiken SW, DiResta GR, et al. Interstitial fluid pressure and blood flow in canine osteosarcoma and other tumors. *Clin Orthop Relat Res* 2001; 385:230–6.
- Salnikov AV, Iversen VV, Koisti M, et al. Lowering of tumor interstitial fluid pressure specifically augments efficacy of chemotherapy. *FASEB J* 2003; 17:1756–8.
- DiResta GR, Lee J, Healey JH, et al. Enhancing the uptake of chemotherapeutic drugs into tumors using an artificial lymphatic system. *Ann Biomed Eng* 2000; 28:556–64.
- Process and device to reduce interstitial fluid pressure in tissue. US patents 5,484,399, 16 January 1996, 6,547,777, 15 April 2003.
- Withrow SJ, Powers BE, Straw RC, et al. Comparative aspects of osteosarcoma: dog versus man. *Clin Orthop Relat Res* 1991; 270:159–68.
- Ehrhart NE, Dernell WS, Hoffmann WE, et al. Prognostic importance of alkaline phosphatase activity in serum from dogs with appendicular osteosarcoma: 75 cases (1990–1996). *J Am Vet Med Assoc* 1998; 213:1002–6.
- Huvos AG, Rosen G, Marcove RC. Primary osteogenic sarcoma: pathologic aspects in 20 patients after treatment with chemotherapy en bloc resection, and prosthetic bone replacement. *Arch Pathol Lab Med* 1977; 101:14–8.
- Zachos TA, Chiaramonte D, DiResta GR, et al. Canine osteosarcoma: treatment with surgery, chemotherapy and/or radiation therapy. The Animal Medical Center, 1993–1998. Proceedings, 19th Annual Veterinary Cancer Society Conference. November 13–19, 1999, Wood's Hole, MA.
- Wong NACS, Willott J, Kendall MJ, Sheffield EA. Measurement of vascularity as a diagnostic and prognostic tool for well-differentiated thyroid tumours: comparison of different methods of assessing vascularity. *J Clin Pathol* 1999; 52:593–7.
- Bergman PJ, MacEwen EG, Kurzman ID, et al. Amputation and carboplatin for treatment of dogs with osteosarcoma: 48 cases (1991 to 1993). *J Vet Intern Med* 1996; 10:76–81.
- Hecquet B, Caty A, Fournier C, et al. Comparison of platinum concentrations in human head and neck tumours following administration of carboplatin, iproplatin or cisplatin. *Bull Cancer* 1987; 74:433–6.
- Takeda S, Ikeba K, Ohkubo T, et al. [Clinical effect of intra-arterial carboplatin-combined chemotherapy for advanced uterine cervical cancer and increased tissue platinum levels with Lipo PGE1 administration before chemotherapy]. *Gan To Kagaku Ryoho* 1996; 23:1697–703.
- Abe I, Suzaki M, Hori K, et al. Some aspect of size-dependent differential drug response in primary and metastatic tumors. *Cancer Metast Rev* 1985; 4:27–39.
- Eriksen J, Tondevold E, Jansen E, et al. Relationship between oxygen and carbon dioxide tensions and acid-base balance in arterial blood and in medullary blood from long bones in dogs. *Acta Orthop Scand* 1979; 50:519–25.
- Li G, Bronk JT, Kelly PJ. Canine bone blood flow estimated with microspheres. *J Orthop Res* 1989; 7:61–7.
- In: Evans HE (eds) *Miller's Anatomy of Dog* 3rd ed. Philadelphia: WB Saunders; 1993.
- Brookhart JM, Parmeggiani PL, Petersen WA, et al. Postural stability in the dog. *Am J Physiol* 1965; 208:1047–57.
- Meyers PA, Heller G, Healey J, et al. Chemotherapy for nonmetastatic osteogenic sarcoma: the Memorial Sloan-Kettering experience. *J Clin Oncol* 1992; 10:5–15.
- Bailey D, Erb H, Williams L, et al. carboplatin and doxorubicin combination chemotherapy for the treatment of appendicular osteosarcoma in the dog. *J Vet Int Med* 2003; 17:199–205.
- Griffey SM, Verstraete FJM, Kraegel SA, et al. Computer-assisted image analysis of intratumoral vessel density in mammary tumors from dogs. *Am J Vet Res* 1998; 59:1238–42.
- Kent MS, Griffey SM, Verstraete FJM, et al. Computer-assisted image analysis of neovascularization in thyroid neoplasms from dogs. *Am J Vet Res* 2002; 63:363–9.
- Simpson JF, Han C, Battifora H, Esteban JM. Endothelial area as a prognostic indicator for invasive breast carcinoma. *Cancer* 1996; 77:2077–85.
- Barbareschi M, Weidner N, Gasparini G, et al. Microvessel density quantification in breast carcinomas. *Appl Immunohistochem* 1995; 3:75–84.

30. Fox SB. Tumour angiogenesis and prognosis. *Histopathology* 1997; 30:294–301.
31. DiResta GR, Aiken SA, Healey JH. Dog osteogenic sarcoma microvasculature visualized with a Spälteholz technique. *Clin Orthop Relat Res* 2004; 426:39–43.
32. Yoshikawa M, Noguchi K, Toda T. Effect of particle sizes in India ink on its use in evaluation of apical seal. *J Osaka Dent Univ* 1997; 31:67–70.
33. Paders TP, Stoll BR, Tooredman JB, et al. Pathology: cancer cells compress intratumour vessels. *Nature* 2004; 452:695.
34. Coomber BL, Denton J, Sylvestre A, et al. Blood vessel density in canine osteosarcoma. *Can J Vet Res* 1998; 62:199–204.
35. DiResta GR, Nathan SS, Manoso M, et al. Population dynamics of cultured human cancer cells are affected by the elevated tumor pressures that exist in vivo. *Ann Biomed Eng* 2005; 33:1270–80.
36. Nathan SS, DiResta GR, Casas-Ganem JE, et al. Elevated physiological tumor pressure promotes proliferation and chemosensitivity in human osteosarcoma cells. *Clin Cancer Res* 2005; 11:2389–97.